MODULE 4

X-Ray Spectroscopy

CONTENTS

Intro:- A technique in which the pattern formed by the diffraction of x-rays when passing through a ~~sub~~ crystalline substance yield information on the lattice structure of the crystal & molecular structure of the substance.

4.1. X-RAY SPECTROSCOPY

4.1.1. Introduction

X-rays have a wavelength of the same order as the inter-atomic spacing in most crystalline substances. X-ray diffraction is thus an ideal way of probing the cell structure of a crystalline substance.

4.1.2. Theory

In this experiment, we mainly consider crystals whose basic or unit cell is cube (of side a). We restrict ourselves to this simple type to make the interpretation easier – the method, however, is most powerful and can be applied generally to all types of crystal structure. There are three basic types of cubic cell – the simple cubic, the face centred cubic and the body centred cubic.

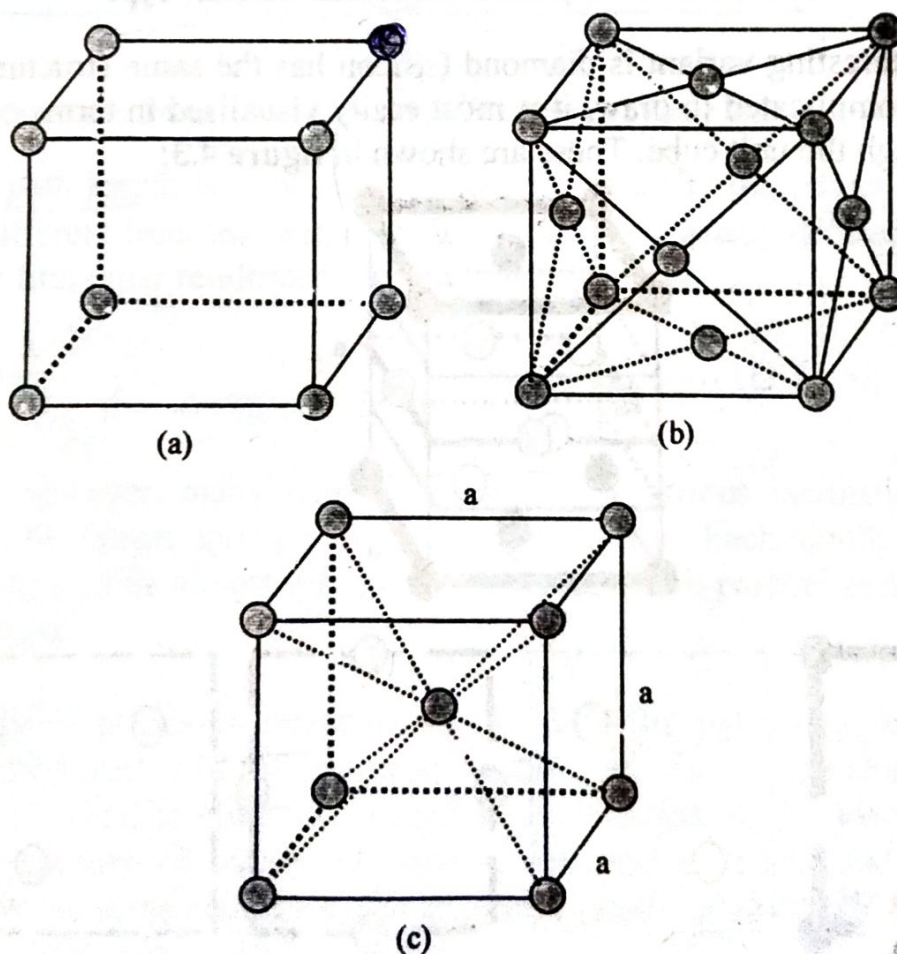The differences in these three types are shown in **figure 4.1**:

Figure 4.1: Cell Structures for Various Crystal Types: (a) Simple Cubic, (b) Face Centred Cubic (FCC), and (c) Body Centred Cubic (BCC)

An interesting variant occurs when a cubic crystal is composed of equal numbers of two types of atoms. The common salt (sodium chloride) is a good example and is shown in **figure 4.2**:
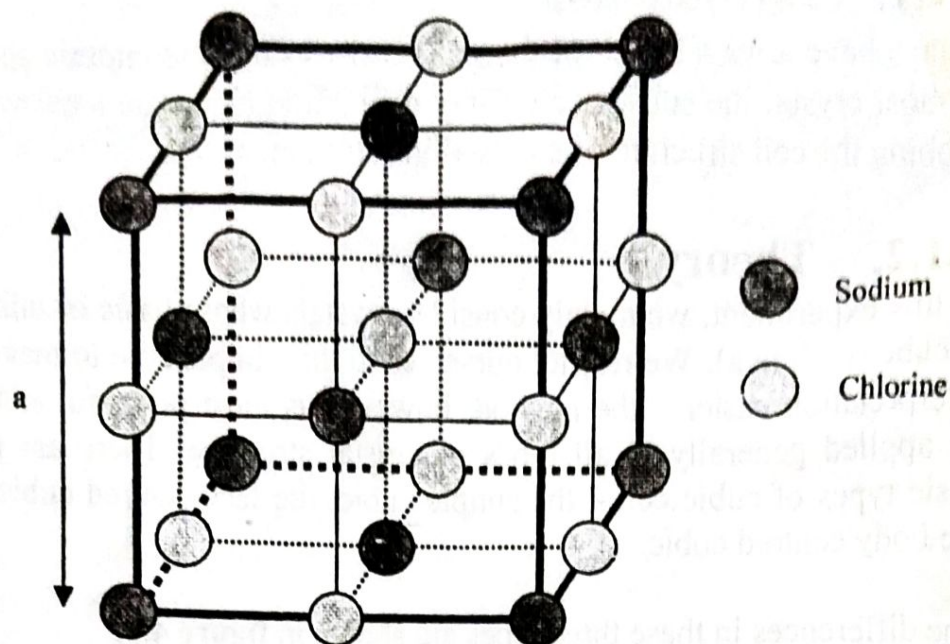
Figure 4.2: Cell Structure for Crystals of the Sodium Chloride Type

Another interesting variant is diamond (silicon has the same structure). Although complicated to draw, it is most easily visualised in terms of 5 slices through the unit cube. These are shown in **figure 4.3**:
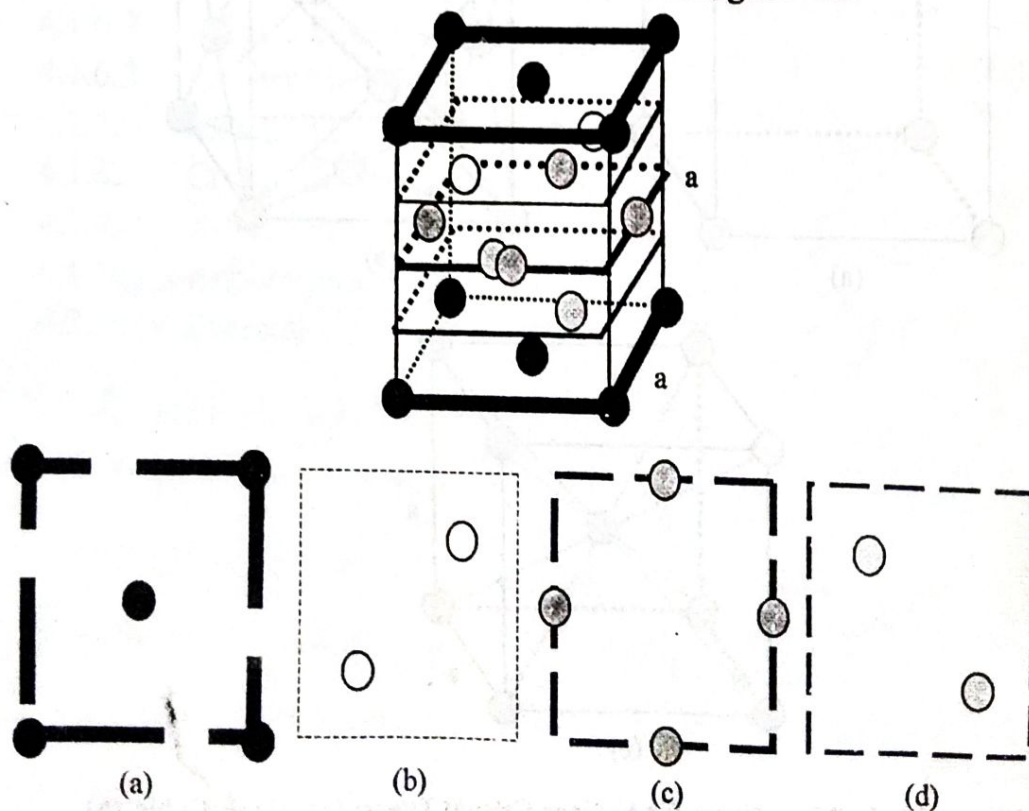

Figure 4.3: Cell Structure for Crystals of the Diamond Type: (a) Top and Bottom Slice, (b) a/4 from Top Slice, (c) a/2 from Top slice, and (d) 3a/4 from Top Slice.

X-Ray Spectroscopy (Module 4)

The technique in this experiment is to use metal samples in the form of wires composed of small crystals orientated in every direction.

The starting point in our reasoning is the Bragg's scattering law which state that x-rays will constructively interfere (and form a high intensity spot on the film) when x-rays scattered from neighbouring planes have path differences differing by an integral number of wavelengths. **Figure 4.4 illustrates this:**
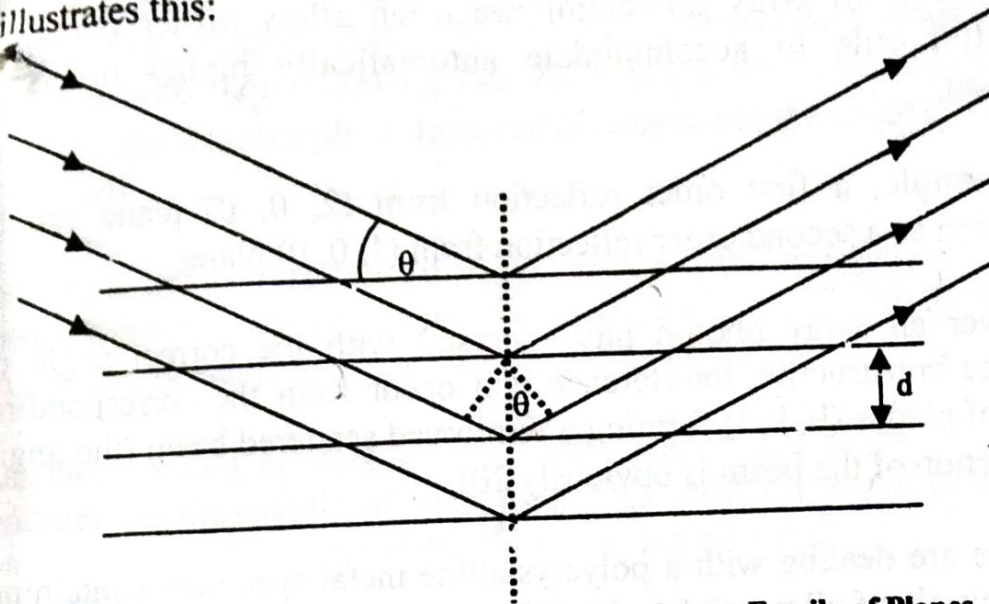

Figure 4.4: Bragg's Reflection of X-Rays from a Family of Planes

The extra path length is $2d \sin\theta = n\lambda$; n is the order of the reflection. The θ is different from the normal angle of incidence usually defined in optics. For first order reinforcement, therefore, we have:

$$\sin\theta = \frac{\lambda}{2d} \qquad\qquad \dots\dots (1)$$

There are, however, many families of planes of various inclinations which can be drawn through the scattering centres. Each family of planes consists of an almost infinite set of members, all parallel and all equally spaced.

Each family of planes is characterised by its Miller indices (h, k, l) which are the inverses of the intercepts on the axes of the plane closest to the origin (in cell coordinates). Thus the Miller indices (0, 0, 1) would described a family of planes all parallel with the xy plane and all separated by the same distance a. For a general family of planes (h, k, l) it is easy to show that:

$$d = \frac{a}{\sqrt{h^2 + k^2 + l^2}} \qquad\qquad \dots\dots (2)$$

so that the Bragg's condition can be written as:

$$\sin^2 \theta = \left(\frac{\lambda}{2a}\right)^2 (h^2 + k^2 + l^2) = \left(\frac{\lambda}{2a}\right)^2 N \qquad \cdots\cdots (3)$$

Clearly N must be an integer. **Equation (3)** already covers higher orders of reflection for $N = n^2$. In crystallography Miller indices are usually given in the lowest terms, i.e., their greatest common divisor should be 1. In x-ray diffraction we often allow Miller indices to break this rule to accommodate automatically higher orders of reflection.

For example, a first order reflection from (2, 0, 0) plane can be considered as a second order reflection from (1, 0, 0) plane.

Whenever an x-ray photon hits a crystal with the correct angle of incidence constructive interference will occur from the corresponding family of planes (h, k, l) forming a reinforced scattered beam (the angle of deflection of the beam is obviously 2θ).

Since we are dealing with a polycrystalline metal specimen containing many crystals of all possible orientations, the scattered beams will form a cone (rather than a bright spot) with an opening angle 2θ with respect to the incident beam direction.
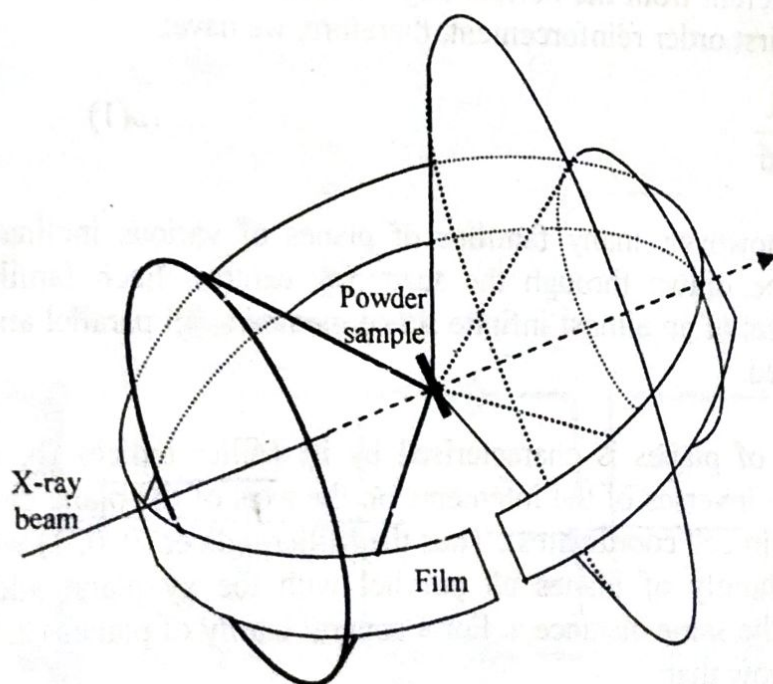
Figure 4.5: Formation of Elliptical Arcs on the Film for a Polycrystalline Sample

The camera used in this experiment utilises a strip of film wrapped around the inner surface (covered with an image intensifier) and enclosing the specimen.

Thus instead of circular rings being seen if the screen is flat perpendicular to the incident beam direction, we see ellipsis or two optical arcs for each value of N. The aim is to ascribe a value of N to each ring seen, thus allowing one to estimate the basic cell size, a, (provided the wavelength of the x-ray is known and the value of $\sin^2\theta$ is calculated).

For simple cubical crystals all values of h, k and l are allowed. All N, however, are not allowed as numbers such as 7, 15, 23, 28, 31 and 39, etc., cannot be made up from the sum of three squares.

For face centred crystals we add extra planes due to the additional scatterers in the middle of each face. This results in some destructive interference; so that some further N values are missing.

Let us consider two slices through a face centred crystal perpendicular to the z axis as shown in **figure 4.6:**
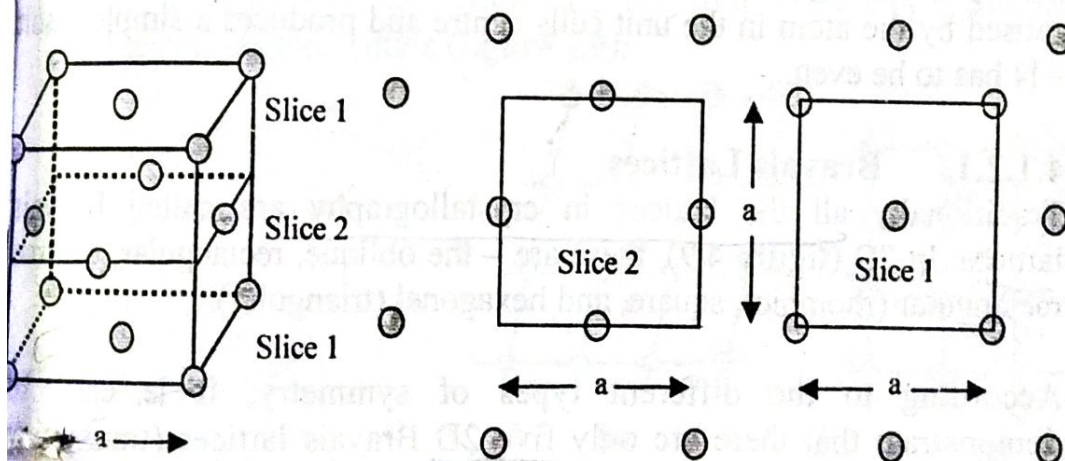
Figure 4.6: In FCC Type of Crystal, the Two Horizontal Slices of the Unit Cell are Just a Different Selections from the Same Pattern of Atoms

The two horizontal slices (slice 1 and 2) have equal numbers of atoms (2) per unit slice area but are separated by half the unit cell size (i.e., by a/2) so there will be destructive interference causing suppression of the reflection hkl = 001 (N = 1). By extension this will mean suppression of hkl = 010 and hkl = 100. If this argument is applied to other planes, the result is that only cases when hkl are all odd and where hkl are all even allowed (i.e., h, k and l must have the same parity).

An interesting effect occurs in crystals like sodium chloride. A pla 111 is entirely occupied by sodium ions and the next 111 plane entirely occupied by chloride ions. This pattern is repeated through t crystal and it causes destructive interference to occur. The interferen is only partially destructive in NaCl as x-ray scattering is strong from the chlorine atoms which have a higher atomic number th sodium.

The result is that the line $N = 3$ (due entirely to hkl = 111) is weak NaCl. The $N = 3$ line is extremely weak (effectively missing) in crysta like NaF and KCl because the component atoms are near neighbours the periodic table. As a general rule, if the planes have atoms of ne equal Z then we see lines with h, k and l all even.

Diamond and silicon lattices have a face centred arrangement of atom with four extra atoms in the cell, arranged as already shown in figur 4.3. The two extra planes cause destructive interference with hkl = 20 ($N = 4$). A similar interference occurs with hkl = 222 ($N = 12$), with h = 420 ($N = 20$) and $N = 30$, 36 and 44. As a consequence, the allowe interval between successive values of N goes 5, 3, 5, 3, etc.

Finally the body centred cubic crystals; destructive interference is caused by the atom in the unit cells centre and produces a simple resul – N has to be even.

4.1.2.1. Bravais Lattices

Traditionally all the lattices in crystallography are called Bravais lattices. In 2D (figure 4.9), these are – the oblique, rectangular, centred rectangular (rhombic), square, and hexagonal (triangular).

According to the different types of symmetry, it is easy to demonstrate that there are only five 2D Bravais lattices (translati groups), but for 3D, there are fourteen Bravais lattices. For periodi structures, besides operations of point symmetry, other symmetry operations involving translations should be considered, they include – pure translations, glide reflections and screw axes (rotations an inversion-rotations).

Pure translations can be easily understood, while the other two, equivalent to a point symmetry operation plus some fractional lattice translation, are more complex. Glide reflections are usually related to translations of t/2, or t/4, where t is the lattice vecto along the glide plane; while N-fold screw rotation is related to

translation vectors $t' = pl/N$, where p is an integer number smaller than N, and l is the translation vector along the rotation axis (figures 4.7 and 4.8):
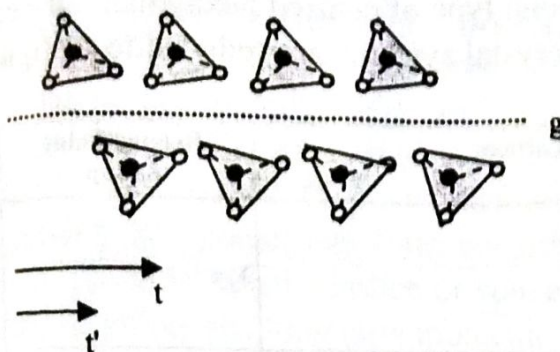

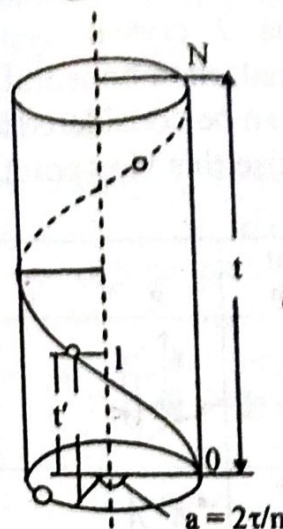**Figure 4.7: Schematic Diagram of a Glide Reflecting Plane**

Figure 4.8: Schematic Diagram of a Screw Axis

Centred lattices are associated with added symmetry operations, such as glide reflections, screw axis operations, etc. In 2D space, the additional operation of the centred lattices is obvious – when compared with the non-centred rectangular lattice, the 2D centred one adds a set of parallel glide reflection lines (a plane changes into a line in the case of 2D), and the translation vector l equals a/2, b/2, so its symmetry is different from the non-centred lattice (figure 4.9):

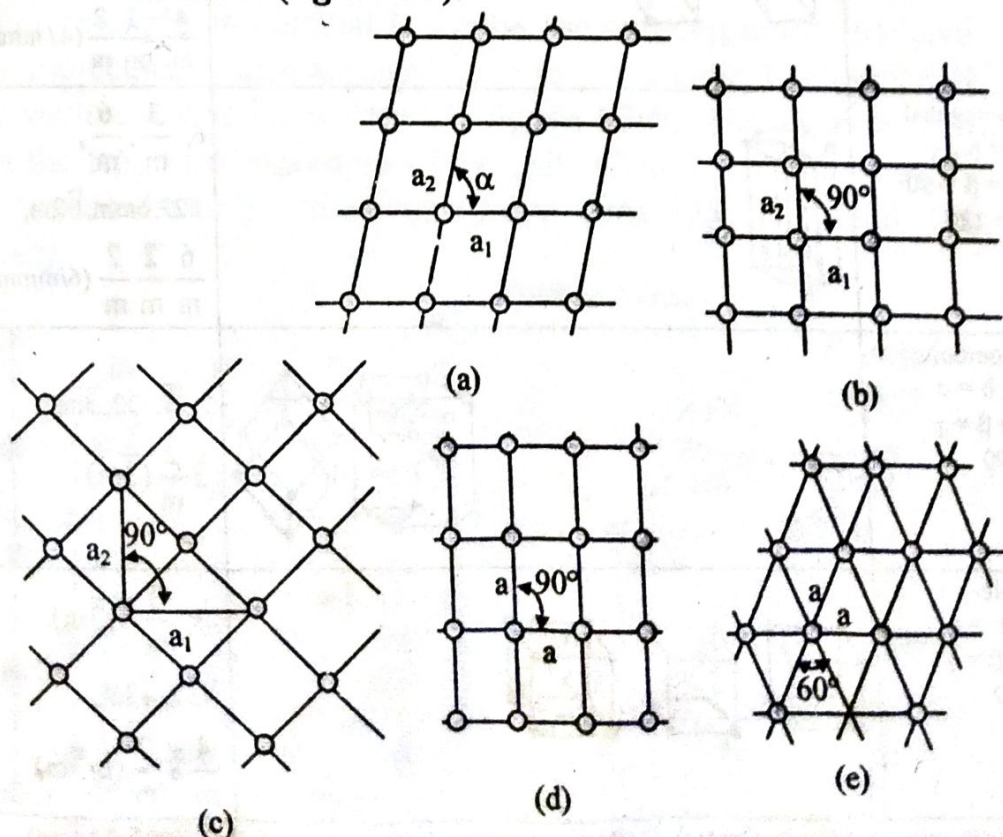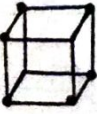**Figure 4.9: 2D Bravais Lattices: (a) Oblique; (b) Rectangular; (c) Rhombic; (d) Square; (e) Hexagonal.**

Although in 3D space the symmetry of lattice is more complex than that of 2D space, the situation is quite similar. 14 Bravais lattices are divided into the 7 crystal systems – Triclinic, monoclinic, orthorhombic, tetragonal, rhombohedral, hexagonal and cubic. The rhombohedral point group can be considered as a special type of centred hexagonal lattice. If we choose this viewpoint, the 7 crystal systems are reduced to 6 (**figure 4.10**):

Crystal System	Type of Lattices						Related Point Group
	P	I	C	F	R		
Triclinic $a \neq b \neq c$ $\alpha \neq \beta \neq \gamma \neq 90$							$1, \tau$
Monoclinic $a \neq b \neq c$ $\alpha = \gamma = 90$ $\beta \neq 90$							$2, m, \dfrac{2}{m}$
Orthorhombic $a \neq b \neq c$ $\alpha = \beta = \gamma = 90$							$222, 2mm,$ $\dfrac{2}{m}\dfrac{2}{m}\dfrac{2}{m}(mmm)$
Tetragonal $a \neq b \neq c$ $\alpha = \beta = \gamma = 90$							$4, \bar{4}, \dfrac{4}{m}422,$ $4mm, \bar{4}2m,$ $\dfrac{4}{m}\dfrac{2}{m}\dfrac{2}{m}(4/mmm)$
Hexagonal $a = b \neq c$ $\alpha = \beta = 90$ $\gamma = 120$							$6, \dfrac{3}{m}, \dfrac{6}{m},$ $622, 6mm, \bar{6}2m,$ $\dfrac{6}{m}\dfrac{2}{m}\dfrac{2}{m}(6/mmm)$
Rhombohedral $a = b = c$ $\alpha = \beta = \gamma$ $\neq 90$							$3, \bar{3}, 32, 3m,$ $\bar{3}\dfrac{2}{m}(\bar{3}m)$
Cubic $a = b = c$ $\alpha = \beta = \gamma$ $= 90$							$23, \dfrac{2}{m}\bar{3}(\bar{3}m).$ $432, \bar{4}3m,$ $\dfrac{4}{m}\bar{3}\dfrac{2}{m}(m\bar{3}m)$

P (Primitive), I (Body Centre), C (Bottom Centre), F (Face Centre), R (Rhombohedron)

Figure 4.10: 14 Kinds of Bravais Lattices

The classification of the Bravais lattices is carried-out by the differences in symmetry, so the types of the lattices coincide with the translation group, i.e., the groups of pure translations.

4.1.2.2.   Space Lattice and Unit Cell

All crystals are polyhedra consisting of regularly repeating arrays of atoms, molecules or ions which are the structural units. A crystal is a homogeneous portion of a solid substance made of regular pattern of structural units bonded by plane surfaces making definite angles with each other. The geometrical form consisting only of a regular array of points in space is called a lattice or space lattice or it can be defined as an array of points showing how molecules, atoms or ions are arranged in different sites, in three-dimensional space. **Figure 4.11(a)** shows a space lattice.

A space lattice can be subdivided into a number of small cells known as unit cells. It can be defined as the smallest repeating unit in space lattice which, when repeated over and over again, results in a crystal of the given substance or it is the smallest block or geometrical figure from which entire crystal can be built up by its translational repetition in three dimensions.

A unit cell of a crystal possesses all the structural properties of the given crystal. For example, if a crystal is a cube, the unit cell must also have its atoms, molecules or ions arranged so as to give a cube. Each unit cell has three vectors a, b and c as shown in **figure 3.3(b)**. The distances a, b and c are the lengths of the edges of the unit cell and angles α, β and γ are the angles between three imaginary axes OX, OY and OZ respectively.

(a) Space Lattice   (b) Unit Cell
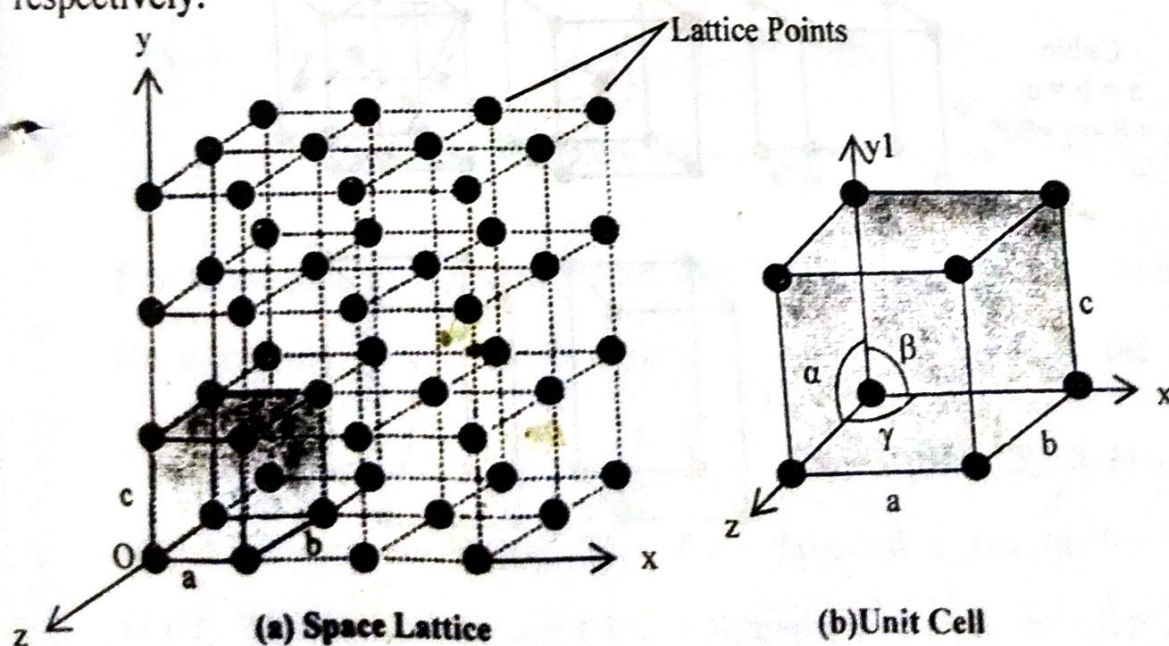
F.gure 4.11: Space Lattice and a Unit Cell (shown by Solid Lines)

4.1.2.3.   Identification of Lattice Points and Planes

To designate the location of any point in the unit cell, a coordinate system is set up with origin at one corner of the unit cell and axes coinciding with a, b, and c edges of the cell. These axes are not necessarily mutually perpendicular.

The position of a point in the cell is specified by giving its coordinates as fractions of the unit-cell lengths a, b, and c. Thus, the point at the origin is 000; the interior lattice point in an I lattice is at $\frac{1}{2}, \frac{1}{2}, \frac{1}{2}$; the r   ıt at the centre of the face bounded by the b and c axes is $0, \frac{1}{2}, \frac{1}{2}$.

4.1.2.3.1.   Miller Indices

The orientation of a crystal plane is described by its **Miller indices** (hkl), which are obtained by the following steps:

1) Find the intercepts of the plane on the a, b, c axes in terms of multiples of the unit-cell lengths a, b, c;

2) Take the reciprocals of these numbers;

3) If fractions are obtained in step 2, multiply the three numbers by the smallest integer that will give whole numbers. If an intercept is negative, one indicates this by a bar over the corresponding Miller index.

Crystal system   Primitive (P)   Body-centred (I)   Face-centred (F)   End-centred (C)

Cubic
a = b = c
α = β = γ =90°

Tetragonal
a = b ≠ c
α = β = γ =90°

Figure 4.11: Space Lattice and a Unit Cell (shown by Solid Lines)
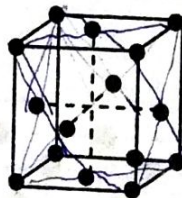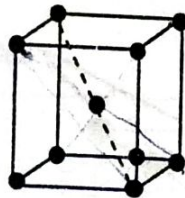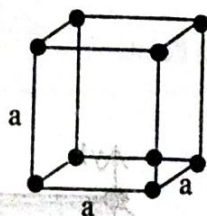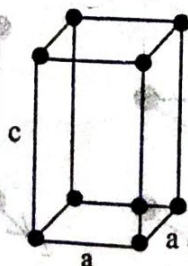
Orthorhombic
$a \neq b \neq c$
$\alpha = \beta = \gamma = 90°$
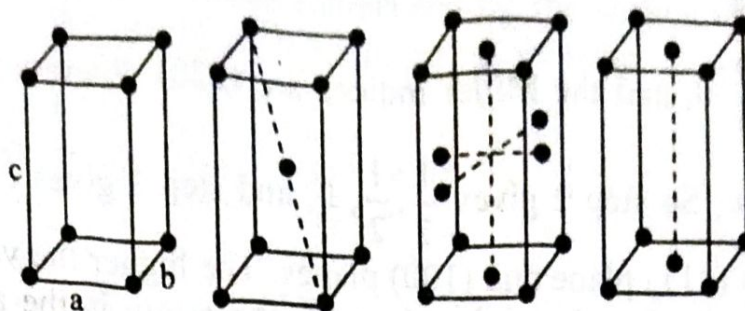
Hexagonal
$a = b \neq c$
$\alpha = \beta = 90°, \gamma = 120°$
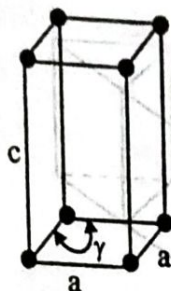
Trigonal (Rhombohedral)
$a = b = c$
$90° \neq \alpha = \beta = \gamma < 120°$
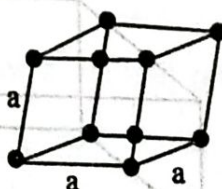
Monoclinic
$a \neq b \neq c$
$\alpha = \gamma = 90°, \beta > 90°$
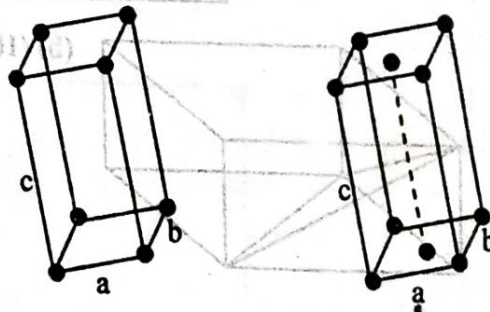
Triclinic
$a \neq b \neq c$
$\alpha \neq \beta = \gamma = 90°$
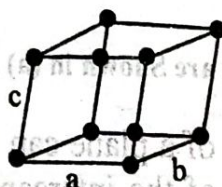
Figure 4.12: Unit Cells of the 14 Bravais Lattices

For example, the shaded plane labelled r in figure 4.13 intercepts the a axis at $\frac{a}{2}$ and the b axis at $\frac{b}{2}$ and lies parallel to the c axis (intercept at ∞). Step 1 gives $\frac{1}{2}, \frac{1}{2}, \infty$. Step 2 gives 2,2,0. Hence the Miller indices are (220). The plane labelled s has Miller indices (110). The plane labelled t has intercepts $\frac{3}{2}a, \frac{3}{2}b$, ∞; step 2 gives

$\frac{2}{3}, \frac{2}{3}$ 0, and the Miller indices are (220). Plane u has intercepts 2a, 2b, ∞; So step 2 gives $\frac{1}{2}, \frac{1}{2}$, 0, and step 3 gives (110). Also shown are a (111, plane and (100) planes. The higher the value of the Miller index h of a plane, the closer to the origin is the a intercept of the plane.

(a) (220) planes

(b) (100) planes

(c) (111) plane
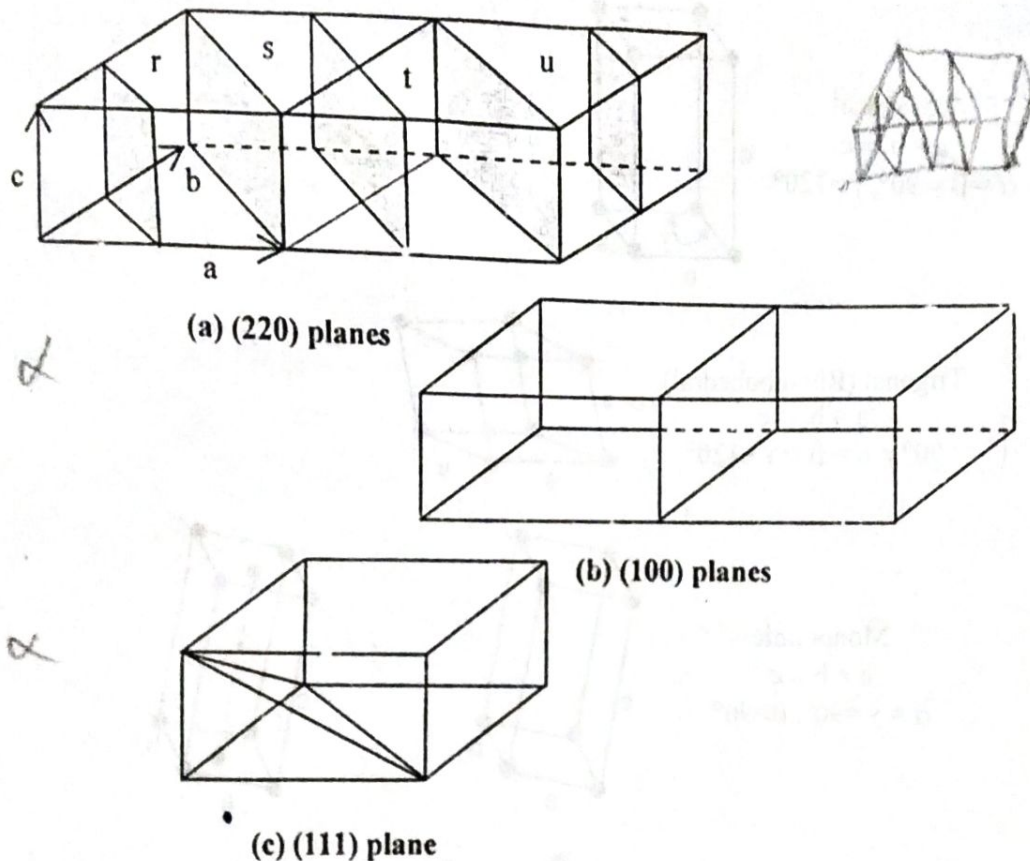
Figure 4.13: Two Unit Cells are Shown in (a) and in (b); One is Shown in (c)

In general, the miller indices of a plane can be expressed as (hkl) where h,k,l refer to the reciprocals of the intercepts expressed in units of the lattice distance, i.e.,

$$h = \frac{a}{\text{Intercepts of the plane along x} - \text{axis}} \quad .....(4)$$

$$k = \frac{b}{\text{Intercepts of the plane along y} - \text{axis}} \quad .....(5)$$

$$l = \frac{c}{\text{Intercepts of the plane along z} - \text{axis}} \quad .....(6)$$

The miller indices (hkl) of any plane give the orientation of the plane in the crystal with reference to its three axes.

4.1.2.2. Separation of Planes

The Miller indices are very useful for expressing the separation of planes. The separation of the (hk0) planes in the square lattice shown in figure 1.40 is given by

$$\frac{1}{d_{hk0}^2} = \frac{h^2 + k^2}{a^2}$$

Or,

$$d_{hk0} = \frac{a}{(h^2 + k^2)^{1/2}} \qquad\qquad .....(7)$$

By extension to three dimensions, the separation of the (hkl) planes of a cubic lattice is given by

$$\frac{1}{d_{hkl}^2} = \frac{h^2 + k^2 + l^2}{a^2}$$

$$d_{hkl} = \frac{a}{(h^2 + k^2 + l^2)^{1/2}} \qquad\qquad .....(8)$$

The corresponding expression for a general orthorhombic lattice is the generalization of this expression:

$$\frac{1}{d_{hkl}^2} = \frac{h^2}{a^2} + \frac{k^2}{b^2} + \frac{l^2}{c^2} \qquad\qquad .....(9)$$
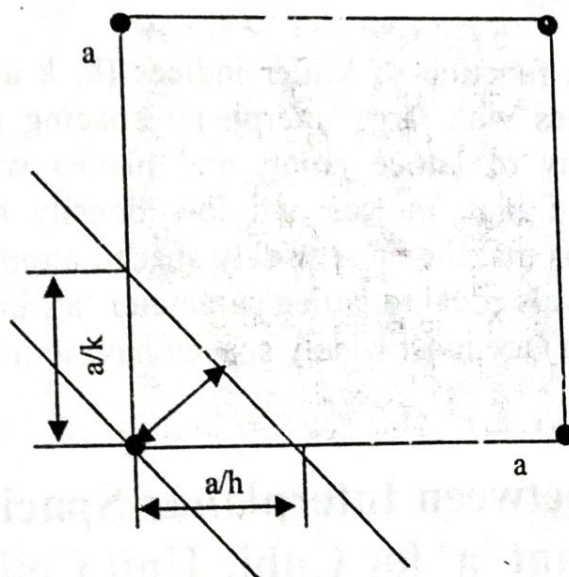
Figure 4.14: Dimensions of a Unit Cell and their Relation to the Plane Passing through the Lattice Points

4.1.3. Interplanar Spacing in Crystal System

Interplanar spacing refers to the magnitude of distance between two adjacent and parallel planes of atoms. Consider cubic unit cell with lattice constant 'a'. The interplannar distance between two adjacent and

126

B. Pharm. Eighth Sem (Pharmaceutical Analysis-III) PTU

parallel planes (1 0 0) as shown in **figure 4.15** is equal to lattice constant, 'a', i.e., $d_{100} = a$. ($d_{hkl} = a$ means interplanar distance between two parallel and adjacent planes having Miller indices h, k, l is equal to a):
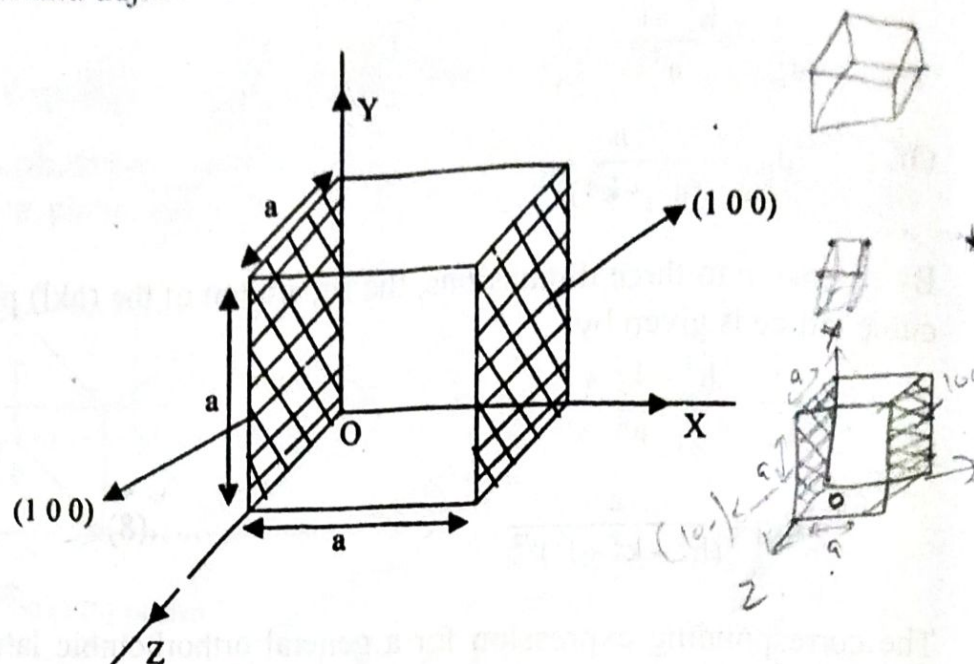
Figure 4.15: Interplanar Spacing in Cubic Crystal

Similarly
$d_{010} = d_{001} = a$

Interplanar spacing is a function of Miller indices (h, k and l) and lattice parameters. Planes with large interplanar spacing have low indices and high density of lattice points and planes with small interplanar spacing have high indices and low density of lattice points. It is quiet obvious that the most widely spaced atomic planes are those spaced at intervals equal to lattice parameter 'a', i.e., planes (1 0 0), (0 1 0) and (0 0 1) are most widely spaced having interplanar distance equal to 'a'.

4.1.4. Relation between Interplanar Spacing 'd' and Lattice Constant 'a' for Cubic Unit Cell

Consider a cubic unit cell with edge length 'a' and plane XYZ with Miller indices h, k, l. The plane XYZ makes intercept of OX, OY and OZ on x, y and z axes respectively as shown in **figure 4.16**.

A plane parallel to XYZ passes through origin and is at a distance 'd' from plane XYZ. A normal OD is drawn from O on plane XYZ such that OD = d. A normal OD makes angle α with x-axis, β with y-axis and γ with z-axis.

Now,

$$OX = \frac{a}{h}, \quad OY = \frac{a}{k}, \quad OZ = \frac{a}{l},$$

$$\cos\alpha = \frac{OD}{OX} = \frac{d}{\frac{a}{h}} = \frac{dh}{a}, \quad \cos\beta = \frac{OD}{OY} = \frac{d}{\frac{a}{k}} = \frac{dk}{a}$$

$$\cos\gamma = \frac{OD}{OZ} = \frac{d}{\frac{a}{l}} = \frac{dl}{a}$$

We know that $\cos^2\alpha + \cos^2\beta + \cos^2\gamma = 1$

$$\left(\frac{dh}{a}\right)^2 + \left(\frac{dk}{a}\right)^2 + \left(\frac{dl}{a}\right)^2 = 1$$

$$\frac{d^2}{a^2}(h^2 + k^2 + l^2) = 1$$

$$d^2 = \frac{a^2}{h^2 + k^2 + l^2}; \quad d = \frac{a}{\sqrt{h^2 + k^2 + l^2}}$$

Clearly interplanar distance 'd' is inversely proportional to the indices h, k, l of the plane.

Figure 4.16

For tetragonal:

$$\frac{1}{d_{hkl}^2} = \frac{h^2 + k^2}{a^2} + \frac{l^2}{c^2}$$

For orthorhombic:

$$\frac{1}{d_{hkl}^2} = \frac{h^2}{a^2} + \frac{k^2}{b^2} + \frac{l^2}{c^2}$$

For hexagonal:

$$\frac{1}{d_{hkl}^2} = \frac{4}{3}\left(\frac{h^2 + hk + k^2}{a^2}\right) + \frac{l^2}{c^2}$$
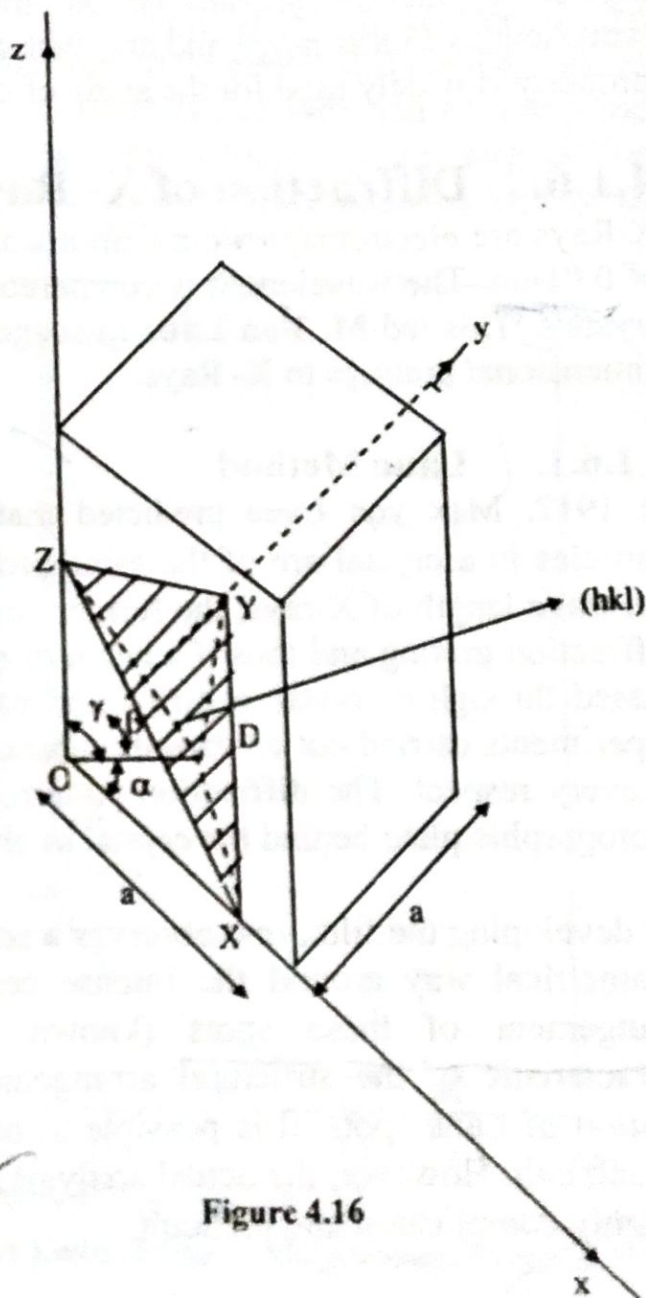
4.1.5. Structure Determination by X-Ray Diffraction

It is well known that, for visible electromagnetic radiation to be diffracted, the spacing between lines in a two-dimensional grating must be of the same order as the wavelength range for light (3900-7800Å). The same principle holds good for diffraction by the three-dimensional grating of the periodic array of atoms in crystals. The typical interatomic spacing in crystals is 2-3Å. So, the wavelength of the radiation used for crystal diffraction should be in the same range. X-rays have wavelengths in this range and are, therefore, diffracted by crystals. The property is widely used for the study of crystal structures.

4.1.6. Diffraction of X-Ray by Crystals

X-Rays are electromagnetic radiations of short wavelength of the order of 0.01nm. The wavelength is comparable with the spacing of atoms in crystals. This led **M. Von Laue** to suggest that crystals can act as three dimensional gratings to X-Rays.

4.1.6.1. Laue Method

In 1912, Max von Laue predicted that since the distances between particles in a crystal are of the same order of magnitude ($\approx 10^{-8}$ cm) as the wave length of X-rays, the former could be used as a 3-dimensional diffraction grating and thus if a beam of non-homogeneous X-rays were passed through a crystal, a diffraction pattern would be observed. The experiments carried out on various substances verified Laue's prediction in every respect. The diffraction pattern can be recorded by placing a photographic plate behind the crystal as shown in **figure 4.17**.

On developing the film, one observes a series of spots arranged in some symmetrical way around the intense central undiffracted beam. The arrangement of these spots (known as **Laue spots**) is highly characteristic of the structural arrangement of the crystal. From the position of Laue spots, it is possible to calculate the size and shape of the unit cell. However, the actual analysis of the Laue diffraction pattern is highly complicated and difficult.

Polychromatic
X-rays

Crystal

Photographic plate   Laue spots
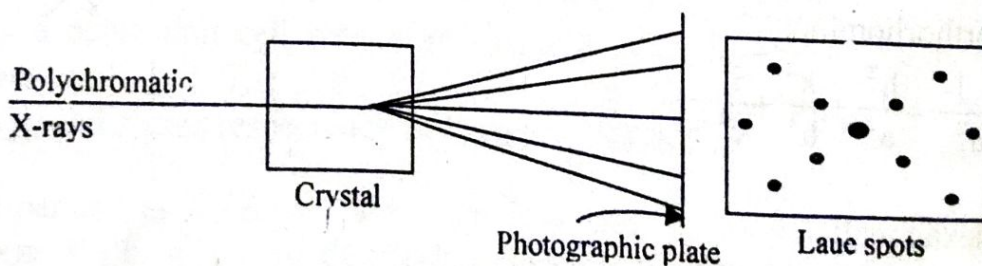
Figure 4.17: Laue Diffraction Pattern

4.1.6.2. Bragg's Equation

When electrons moving at high speed, are directed to a metal target, a small percentage of their kinetic energy is converted into x-rays. The x-rays emitted by the target consist of a continuous range of wavelengths, called white radiation, by analogy with white light consisting of a range of wavelengths. The minimum wavelength in the continuous spectrum is inversely proportional to the applied voltage which accelerates the electrons towards the target. If the applied voltage is sufficiently high, in addition to the white radiation, a characteristic radiation of a specific wavelength and high intensity is also emitted by the target. The radiation emitted by a molybdenum target at 35kV includes both types of radiation as illustrated in figure 4.18:
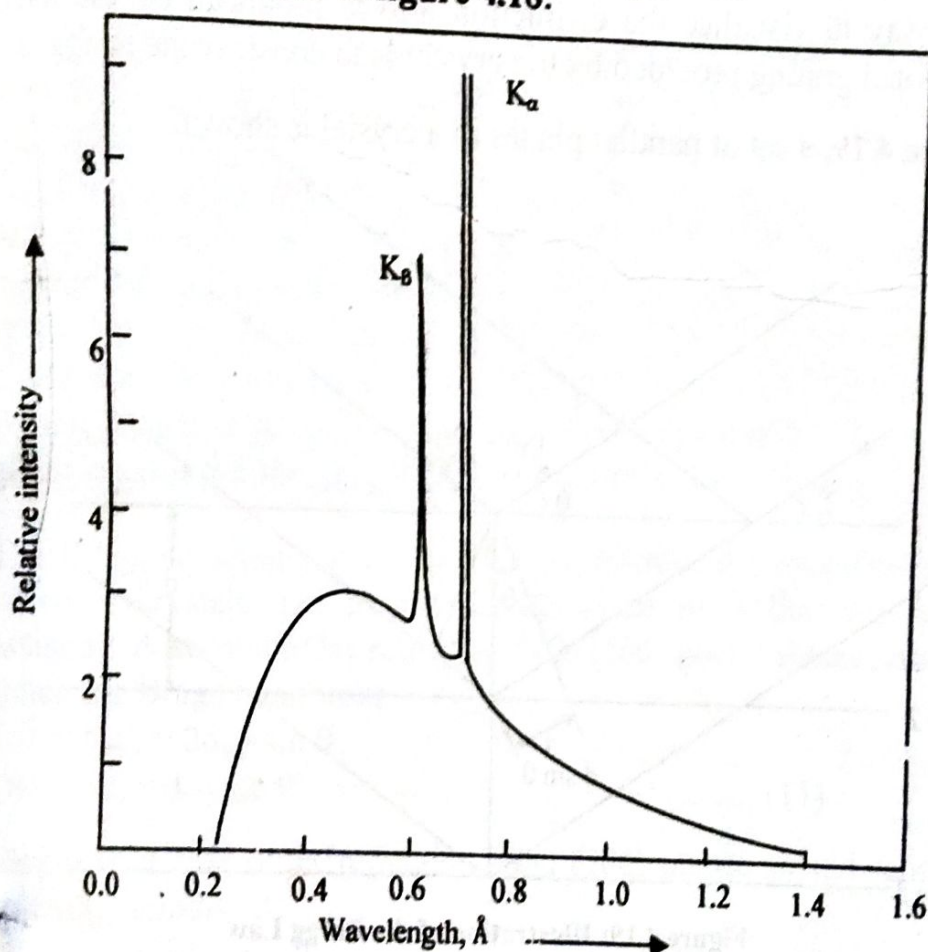
Figure 4.18: Spectrum of X-Rays Emitted from a Molybdenum Target at 35kV

In spectroscopic notation, the characteristic radiations are named K_α, K_β, L_α, etc. K_α radiation has a high intensity and is commonly used in diffraction studies. The wavelengths of this radiation for typical target metals are given in table 4.1:

Table 4.1: Wavelengths of K_α Radiation for Typical Target Metals

Target Metal		Mo	Cu	Co	Fe	Cr
K_α wavelength,	Å	0.71	1.54	1.79	1.94	2.29
	nm	0.071	0.154	0.179	0.194	0.229

A beam of x-rays directed at a crystal interacts with the electrons of the atoms in the crystal. The electrons oscillate under the impact and become a new source of electromagnetic radiation. The waves emitted by the electrons have the same frequency as the incident x-rays. The emission is in all directions. As there are millions of atoms in a crystal, the emission in a particular direction is the combined effect of the oscillations of electrons of all the atoms. The emissions will be in phase and reinforce one another only in certain specific directions, which depend on the direction of the incident x-rays, their wavelength as well as the spacing between atoms in the crystal. In other directions, there is destructive interference of the emissions from different sources. The easiest way to visualise the diffraction effects produced by the three-dimensional grating provided by the crystal is to consider the Bragg law.

In **figure 4.19**, a set of parallel planes in a crystal is shown:
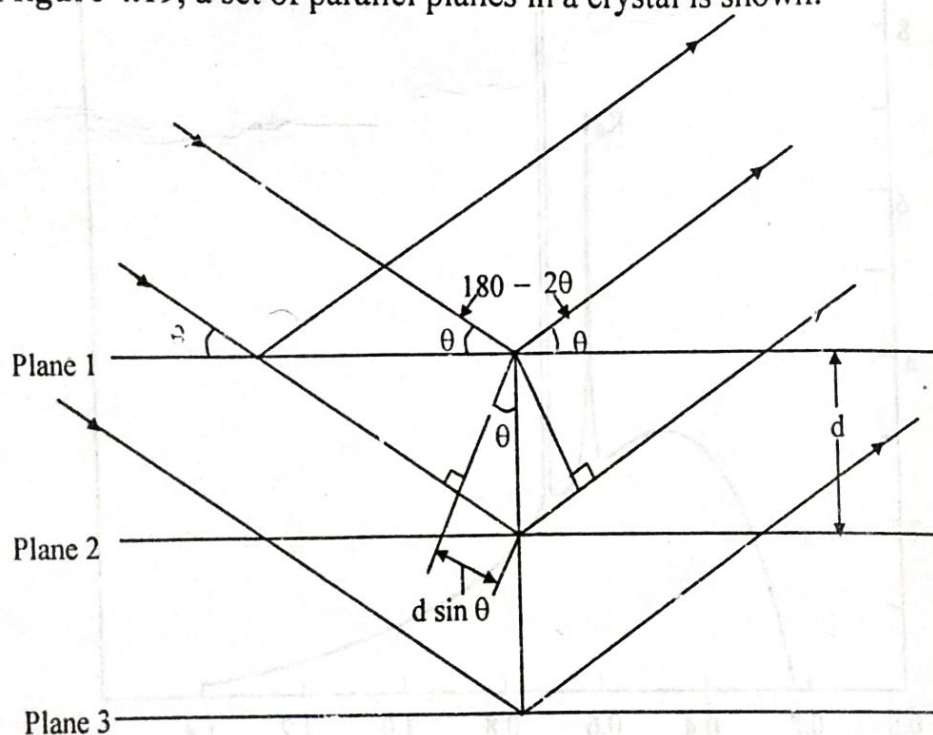
Figure 4.19: Illustration of the Bragg Law

A beam of x-rays of wavelength λ is directed towards the crystal at an angle θ to the atomic planes. In Bragg law, the interaction described above between x-rays and the electrons of the atoms is visualised as a process of reflection of x-rays by the atomic planes. This is an equivalent description of the diffraction effects produced by a three-dimensional grating. The atomic planes are considered to be semi-transparent, i.e., they allow a part of the x-rays to pass through and reflect the other part, the incident angle θ (called the Bragg angle) being equal to the reflected angle Referring to **figure 4.19**, there is a path difference between rays reflected from plane 1 and the adjacent plane 2

in the crystal. The two reflected rays will reinforce each other, only when this path difference is equal to an integral multiple of the wavelength. If d is the interplanar spacing, the path difference is twice the distance d sin θ, as indicated in **figure 4.19**. The Bragg condition for reflection can therefore be written as:

$$n\lambda = 2d \sin \theta \qquad \ldots\ldots (10)$$

where, n = an integer

λ = wavelength of the x-rays used.

A first order reflection is obtained, if n = 1; a second order reflection occurs if n = 2, and so on.

As sin θ has a maximum value of 1, for a typical value of interplanar spacing of 2Å, **equation (10)** gives the upper limit of λ for obtaining a first order reflection as 4Å. There will be no reflection if λ is greater than 4Å. λ can be reduced indefinitely, obtaining reflections from other sets of planes that have spacing less than 2Å as well as an increasing number of higher order reflections. A very small wavelength of the order of 0.1Å is not necessarily an advantage as it tends to produce other effects such as knocking off electrons from the atoms of the crystal and getting absorbed in the process. The wavelengths of the K_α radiation given in **table 4.1** for typical target metals lie in the right range.

The Bragg equation can be used for determining the lattice parameters of cubic crystals. Let us first consider the value that n should be assigned. A second order reflection from (100) planes should satisfy the following Bragg condition:

$$2\lambda = 2d_{100} \sin \theta$$

Or $\quad \lambda = d_{100} \sin \theta \qquad\qquad \ldots\ldots (11)$

Similarly, a first order reflection from (200) planes should satisfy the following condition:

$$\lambda = 2d_{200} \sin \theta \qquad\qquad \ldots\ldots (12)$$

The interplanar spacing of (100) planes is twice that for (200) planes. So **equations (11)** and **(12)** are identical. For any incident beam of x-rays, the Bragg angle θ would be the same, as the two sets of planes in question are parallel. As **equations (11) and (12)** are identical, the two reflections will superimpose on each other and cannot be distinguished. By a similar argument, it can be shown that the third order reflection from (100) planes will superimpose on the first order reflection from (300) planes. In view of such superimposition, there is no need to consider the variations in n separately; instead, we take n to be unity for

B. Pharm. Eighth Sem (Pharmaceutical Analysis-III) PTU

132

all reflections from parallel sets of planes such as (100), (200), (300), (400), etc. **For example,** in a crystal it may turn out that there is no (200) plane with atoms on it. Then, what is designated as a (200) reflection actually refers to the second order reflection from (100) planes.

4.1.6.3. Powder Method

The powder method is a widely used experimental technique for the routine determination of crystal structures. It is highly suitable for identification and for determination of the structures of crystals of high symmetry. Here, a monochromatic x-ray beam, usually of K_α radiation, is incident on thousands of randomly oriented crystals in powder form. The powder camera, called the **Debye-Scherrer camera,** consists of a cylindrical cassette, with a strip of photographic film positioned around the circular periphery of the cassette. The powder specimen is placed at the centre of the cassette in a capillary tube or pasted on a thin wire. The tube, the wire and the paste material must be of some non-diffracting substance such as glass or glue. The x-ray beam enters through a small hole, passes through the powder specimen and the unused part of the beam leaves through a hole at the opposite end. The geometry of the powder method is illustrated in **figure 4.20:**
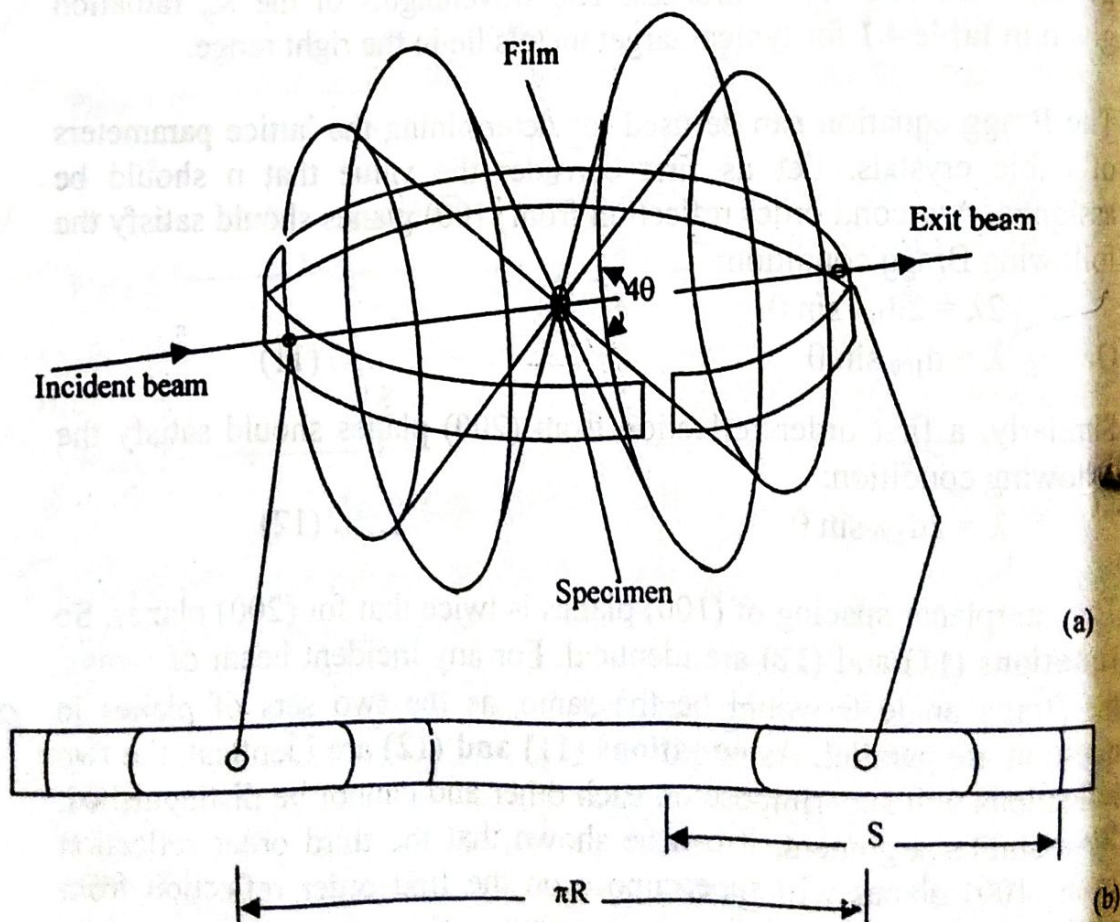

Figure 4.20: Geometry of the Powder Method

Consider a set of parallel crystal planes making an angle θ with the incident direction. When this angle satisfies the Bragg equation, there is reflection. By virtue of the large number of randomly oriented crystals in the powder, there are a number of possible orientations of this set of planes in space for the same angle θ with the incident direction. So the reflected radiation is not just a pencil beam like the incident one; instead, it lies on the surface of a cone whose apex is at the point of contact of the incident radiation with the specimen. Also, the interplanar spacing d being the same for all members of a family of crystal planes, they all reflect at the same Bragg angle θ, all reflections from a family lying on the same cone.

After taking n = 1 in the Bragg equation, there are still a number of combinations of d and θ that would satisfy the Bragg law. For each combination of d and θ, one cone of reflection must result and, therefore, many cones of reflection are emitted by the powder specimen. If the reflected cones were recorded on a flat film placed normal to the exit beam, they will be in the form of concentric circles. In the powder camera, however, only a part of each reflected cone is recorded by the film strip positioned at the periphery of the cylindrical cassette. The recorded lines from any cone are a pair of arcs that form part of the circle of intersection. When the film strip is taken out of the cassette and spread out, it looks like **figure 4.20b**.

The angle between a reflected line lying on the surface of the cone and the exit beam is 2θ. Therefore, the angle included at the apex of the cone is twice this value, 4θ, **figure 4.20a**. When the Bragg angle is 45°, the cone opens out into a circle and reflection at this angle will make a straight line intersection with the film strip at the midpoint between the incident and the exit points in **figure 4.20b**. When the Bragg angle is greater than 45°, back reflection is obtained, i.e., the reflected cones are directed towards the incident beam. Bragg angles upto the maximum value of 90° can be recorded by the film of the powder camera, which is not possible on a flat film placed in front of the exit beam.

The exposure in a powder camera must be sufficiently long to give reflected lines of good intensity. The exposure time is usually a few hours. After the film is exposed and developed, it is indexed to determine the crystal structure. It is easily seen that the first arc on either side of the exit point corresponds to the smallest angle of reflection. The pairs of arcs beyond this pair have larger Bragg angles and are from planes of smaller spacings, recall that $d = \lambda/(2\sin\theta)$. The distance

between any two corresponding arcs on the spread out film is termed S
figure 4.20b. S is related to the radius of the powder camera R:

$$S = 4R\theta \qquad \ldots\ldots (13)$$

where θ is the Bragg angle expressed in radians. For easy conversion of
the distance S measured in mm to Bragg angle in degrees, the camera
radius is often chosen to be 57.3mm, as 1 rad = 57.3°.

In the powder method, the intensity of the reflected beam can also be
recorded in a diffractometer, which uses a counter in place of the film to
measure intensities. The counter moves along the periphery of the
cylinder and records the reflected intensities against 2θ. Peaks in the
diffractometer recording (**figure 4.21**) correspond to positions where the
Bragg condition is satisfied:
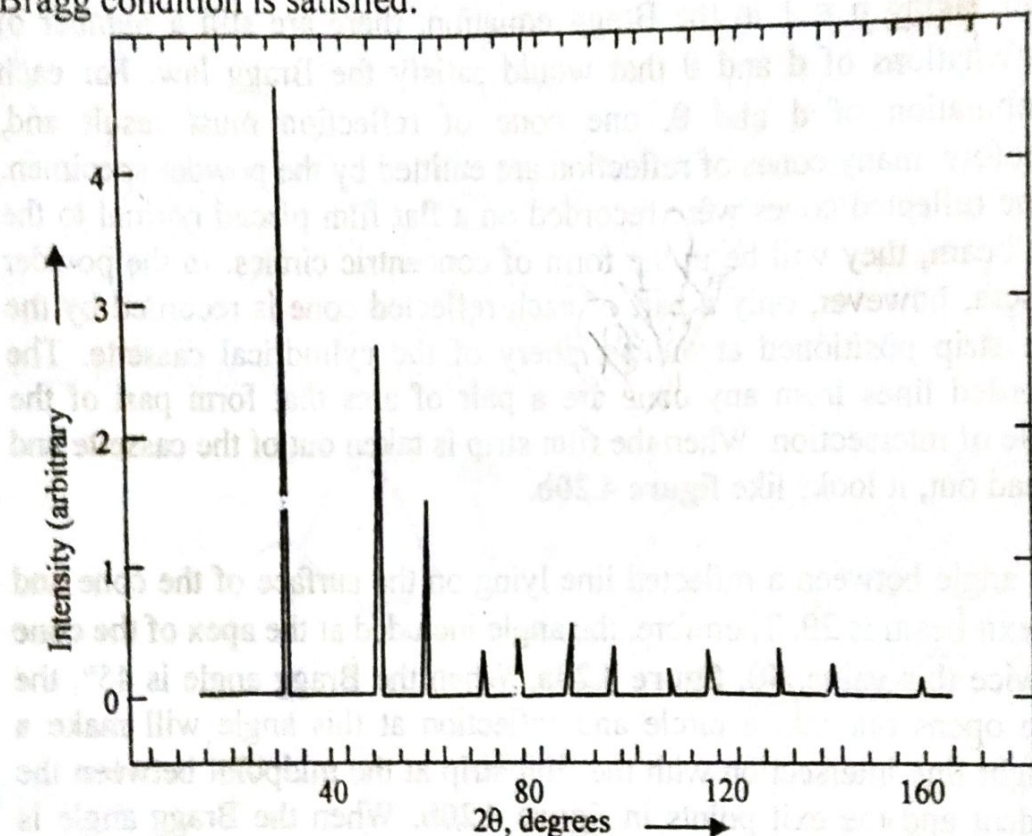
Figure 4.21: Tracing from a Diffractometer

4.1.7. Structure Determination

The determination of a complex crystal structure is often time-
consuming, requiring a lot of patience and ingenuity. A step-by-step
procedure is followed in such cases, first determining the macroscopic
symmetry of the crystal, then the space lattice and its dimensions, and
finally the atomic arrangement within the unit cell. Measurement of the
density of the crystal and the chemical composition also assist the
process of structure determination. In simple crystals of high symmetry,
the space lattice and its dimensions can be determined relatively easily.
If the crystal is monoatomic, the space lattice together with the lattice

parameters is a complete description of the crystal structure. If, on the other hand, the basis is two or more atoms per lattice point, the number and distribution of atoms within the unit cell can be determined only from quantitative measurements of the reflected intensities. For such measurements, the recording from a diffractometer is more useful than the pattern obtained from a powder camera.

Combining **equation (11)** for the interplanar spacing d with the Bragg equation, we obtain:

$$Sin^2\theta = \frac{\lambda^2}{4a^2}(h^2 + k^2 + l^2) \quad ...... (14)$$

n is assumed to be 1 for reasons already outlined. θ-values can be determined from a powder pattern using **equation (13)**. Since monochromatic radiation is used in the powder technique, the value of λ is known. Then, the unknowns in **equation (14)** are the Miller indices of the reflecting planes that correspond to the measured angles of reflection. For a given cubic lattice, it is possible to list all combinations of h, k and l and arrange $(h^2 + k^2 + l^2)$ in increasing order which will also be the increasing order of θ values, as seen from **equation (14)**. The $sin^2 \theta$ values will be in the same ratio as $(h^2 + k^2 + l^2)$, if the assumed and actual lattices coincide.

4.1.8. Crystal Geometry & Structure Determination

The distinction between lattices of the cubic system is possible by using the fact that not all combinations of $(h^2 + k^2 + l^2)$ lead to reflection for a given lattice. Consider the first order reflection from the planes of a BCC crystal. These planes are the faces of the unit cube and contain the 'corner' atoms of the cube, **figure 4.22**:
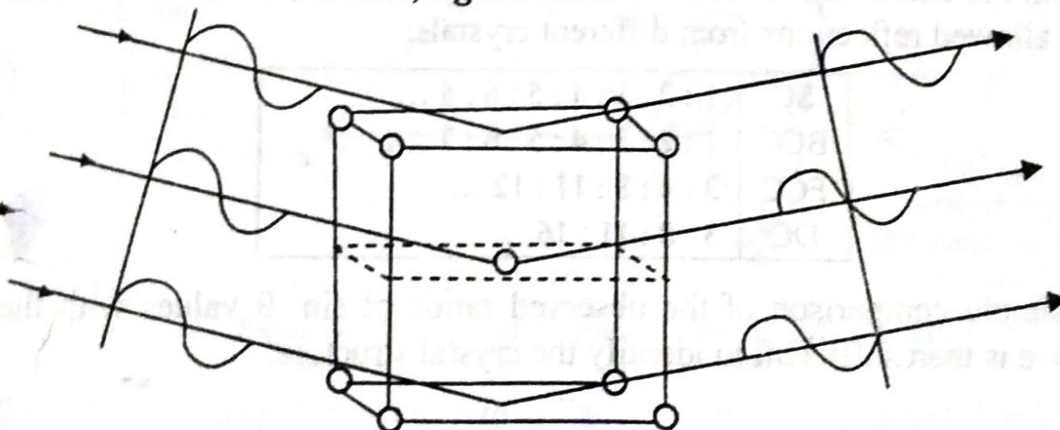

Figure 4.22: Reflection is Absent for a BCC Crystal, as Reflection from the Corner Atoms is Exactly Cancelled Out by that from Body Centred Atoms

The path difference between reflected beams from two adjacent planes is one full wavelength and, therefore, the reflected beams are in phase.

The midway parallel plane between these two planes contains the body centred atoms. It is easily seen that the reflection from this midplane will be out of phase by exactly half of a wavelength with the reflections, figure 4.22.

As the effective number of body centred atoms is equal to the effective number of corner atoms in a BCC crystal, the intensity of the reflected beams from atoms at these two locations will be exactly equal. The phase difference $\lambda/2$ then results in a net zero reflected intensity. (Body centred atoms and body corner atoms, are defined only in a relative sense and are interchangeable.) There is thus no first order reflection from planes in BCC crystal. A second order reflection from planes is possible, but this will superimpose on the first order reflection from planes.

By following a similar reasoning, it is possible to derive extinction rules for different cubic crystals, as given table 4.2:

Table: 4.2: Extinction Rules for Cubic Crystals

Crystal	Reflections are Allowed
SC	For all values of $(h^2 + k^2 + l^2)$.
BCC	For even values of $(h + k + l)$.
FCC	When h, k and l are all odd or all even.
DC	When h, k and l are all odd, or when all are even, $(h + k + l)$ should be divisible by four.

In the above, zero is taken as an even number. The Diamond Cubic (DC) crystal is based on the FCC space lattice, with a basis of two atoms per lattice point.

From the extinction rules, we can derive the ratio of $(h^2 + k^2 + l^2)$ values for allowed reflections from different crystals:

SC	1 : 2 : 3 : 4 : 5 : 6 : 8 ...
BCC	1 : 2 : 3 : 4 : 5 : 6 : 7 ....
FCC	3 : 4 : 8 : 11 : 12 ...
DC	3 : 8 : 11 : 16 ...

A simple comparison of the observed ratios of $\sin^2 \theta$ values with the above is then sufficient to identify the crystal structure.

## 4.1.9. X-Ray Diffraction Pattern of Cubic System (NaCl Powder)

The formation of NaCl crystal can be explained in the following manner. The two ions form one ion-pair of opposite charges by the electrostatic force of attraction. Each of the ions has a strong residual

field around it and will naturally attract another ion-pair much in the same way as two magnets attract each other, i.e., a cluster is formed. Two clusters combine together to give a unit cell. Finally large number of unit cells unite together to form three-dimensional cubic crystal.

An examination of NaCl crystal **figure 4.23** confirms the following points:

1) Each Na^+ ion is surrounded by six Cl^- ions at the corners of a regular octahedron and similarly each Cl^- ion is surrounded by six Na^+ ions. It is, therefore, termed as 6: 6 arrangements. The radius ratio $\left| r_{Na}^+ / r_{cl}^- = 0.95/1.81 = 0.524 \right|$ suggests that coordination number of each ion is six.

2) In the octahedral structure, Cl^- ions may be regarded as having a cubic closed packed (ccp) arrangement in which all octahedral holes are filled by Na^+ ions.
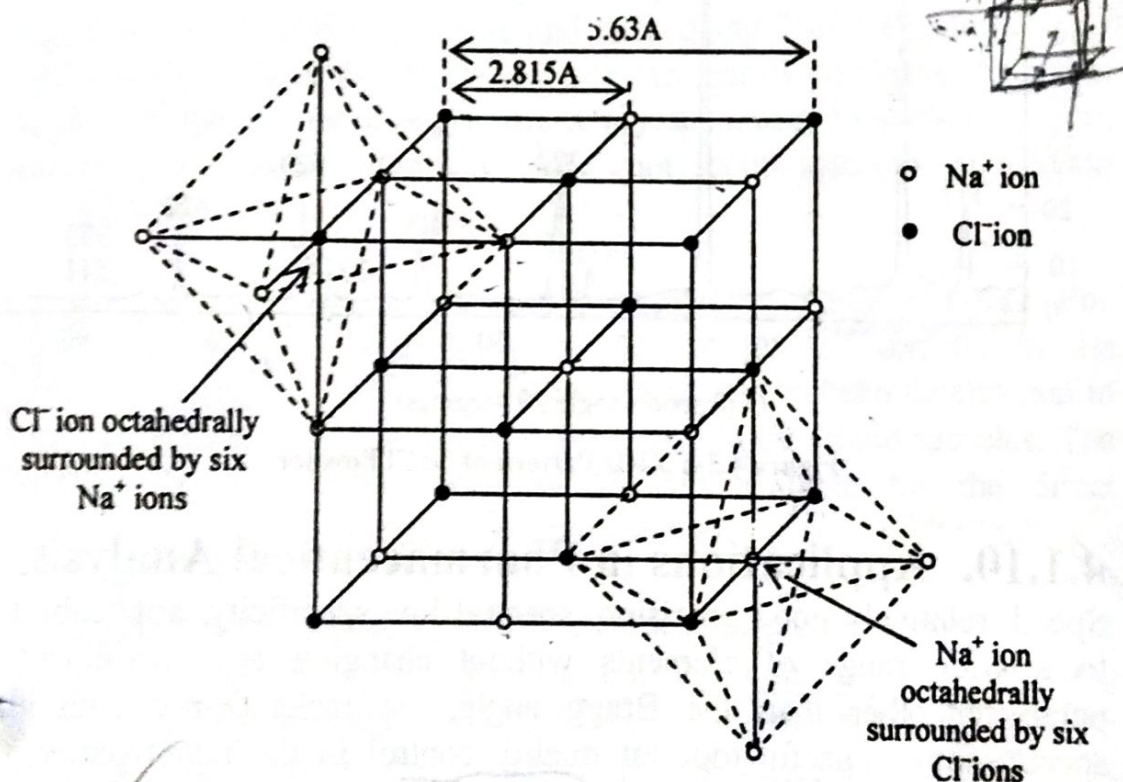
Figure 4.23: Unit Cell Representation of NaCl Structure

3) The distance between two adjacent ions of different kinds is equal to 2.815 Å. Thus, two ions are not touching each other as the sum of their ionic radii is 2.76 Å (0.95 + 1.81 = 2.76). This type of structure is possessed by most of the alkali metal halides (KCl, NaI), alkaline earth metal oxides and AgF, AgCl, AgBr, NH_4Cl, NH_4Br, etc.

The unit cell of sodium chloride had four sodium ions and four chloride ions.

i) Number of sodium ions $= 12$ (at the edge centres) $\times \dfrac{1}{4} + 1$ (at body centre) $= 4$

ii) Number of chloride ions $= 8$ (at the corners) $\times \dfrac{1}{8} + 6$ (at face centres) $\times \dfrac{1}{2} = 4$
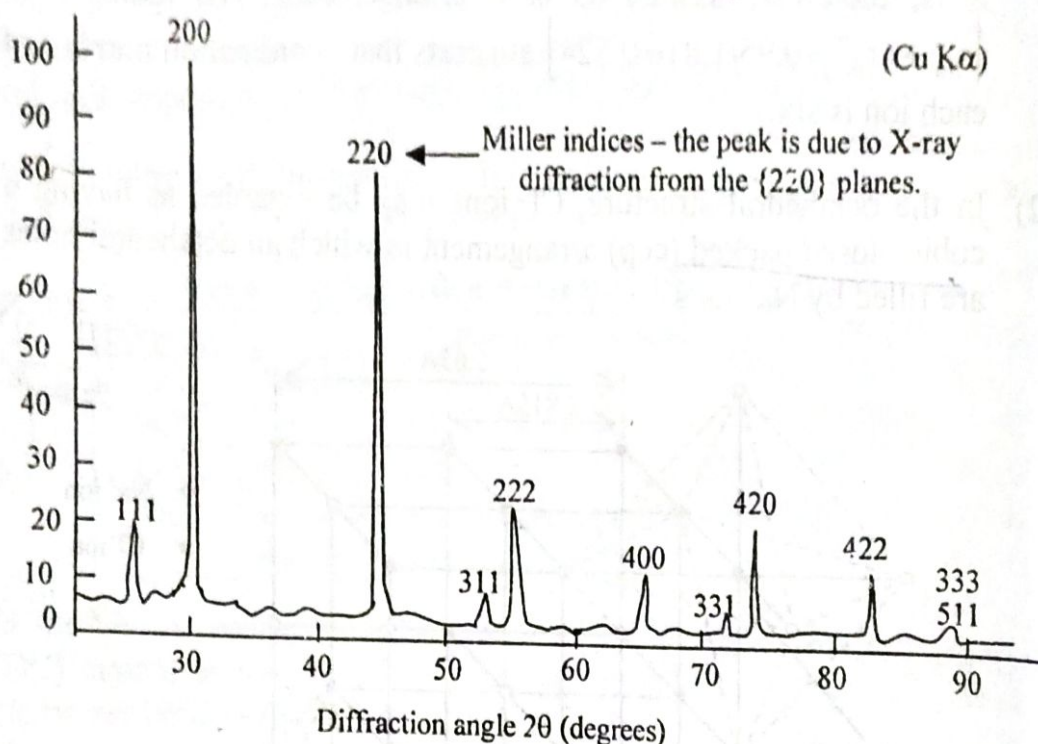

Figure 4.24: XRD Pattern of NaCl Powder

4.1.10. Applications in Pharmaceutical Analysis.

Speed, relatively good precision, spectral line specificity, applicability to a wide range of elements without changing any instrumental parameter other than the Bragg angle, etc make X-ray emission spectroscopy a useful tool for quality control in the manufacture of metals and alloys. The method has also been used widely for mineral analysis and also in the determination of closely related constituents of rare earth minerals.

X-ray emission provides a convenient means of analysis for high alloy steels and for heat resistant alloys of Cr-Ni-Co type. Analysis of low percentages is limited by the absorption of the emitted radiation of the element by the materials of the specimen. Samples having an element of

high atomic weight will absorb a higher percentage of radiation than would be absorbed by a light element (having low atomic weight). Thus nickel in an aluminium alloy can be determined with greater sensitivity than nickel in steel or silver or lead alloy, where the absorption of NiKα radiation is high.

A particularly important elemental analytical application of this technique is the direct determination of lead in gasoline.

This has been widely used to measure the volume of liquids in closed vessels or pipes without opening or breaking the vessels or pipes.

Birks and Brooks have also applied X-ray emission in the determination of hafnium in zirconium and tantalum in niobium. Emission methods have also been applied successfully in trace analysis.

Vassos, Hirsch and Letterman have determined various metals to a concentration of a fraction of $1\mu g \, mL^{-1}$ in a 90 minute electrolysis onto a cathode of pyrolusite graphite and subsequent X-ray examination of the cathode surface. Pyrolusite graphite can readily be cleaved into thin layers suitable for mounting in the X-ray apparatus. Moreover, carbon, having low atomic number does not contribute to significant background.

X-ray emission methods are readily adapted to liquid samples. **For example,** lead and bromine have been determined directly in the aviation gasoline samples. Ca, Ba and Zn have also been determined in lubricating oils by excitation of fluorescence in the liquid samples. The method has also been found to be very suitable for the direct determination of the pigments in paint samples.

Emission X-ray methods have been used worldwide for research and for control analysis of major, minor and trace elements. This increasing interest in emission methods is probably due to wide applicability of X-rays for rapid quantitative analysis. X-ray emission methods have proved to be of immense applicability in such analytical problems as iron in blood, calcium in cement, titanium in paper products, chromium in glass and selenium in plant materials.

The most recent development in emission applications has been the on-stream process control of metallurgical systems. **For example,** addition of floatation reagents to a sphalerite concentrate is controlled by on stream analysis of heads, concentrates and tailings.